

# Capacity and SKR tradeoff in coexisting classical and CV-QKD metropolitan-reach optical links

Çağla Özkan<sup>1,\*</sup>, Lucas Alves Zischler<sup>2</sup>, Kadir Gümüş<sup>1</sup>, João dos Reis Frazão<sup>1</sup>, Cristian Antonelli<sup>2</sup>, and Chigo Okonkwo<sup>1</sup>

<sup>1</sup>High-capacity Optical Transmission Laboratory, Eindhoven University of Technology, The Netherlands

<sup>2</sup>Department of Physical and Chemical Sciences, University of L'Aquila, L'Aquila, Italy

\*c.o.ozkan@tue.nl

**Abstract:** We demonstrate power-regime-dependent guardband optimization for quantum-classical coexistence in metropolitan DWDM. Quantum channel at band-edge with 100–150 GHz guardbands achieves 108% SKR improvement at  $-1.5$  dBm/ch, incurring 3.4% capacity loss versus 6.8% for band-center. © 2026 The Author(s)

## 1. Introduction

Quantum Key Distribution (QKD) is rapidly maturing to provide physical layer security during key generation. However, the need for dedicated dark fiber infrastructure limits widespread deployment [1, 2]. Continuous-variable (CV) QKD, with its enhanced noise tolerance compared to discrete-variable (DV) QKD, enables coexistence with classical traffic in metropolitan Dense Wavelength-Division Multiplexing (DWDM) networks over distances reaching up to 120 km with local local oscillator (LLO) schemes [3]. Nevertheless, the coexistence of weak quantum signals with strong classical channels introduces nonlinear interference, mainly from Spontaneous Raman Scattering (SpRS) and Four-Wave Mixing (FWM) [4].

Early studies on coexistence have identified SpRS as the dominant noise source at long distances. In these studies, CV-QKD operation with co-propagating classical powers up to 11.5 dBm over 25 km was demonstrated [5]. However, at metropolitan distances (e.g., 10–25 km) with high channel loading, FWM's cubic power dependence causes it to dominate over SpRS [6, 7]. Although other studies have recently assessed the feasibility of coexistence and identified spectral dependencies using split-step Fourier simulations [8], systematic design guidelines for guardband allocation across power regimes and quantitative SKR-capacity tradeoff analysis for metropolitan DWDM deployment remain to be developed.

This work addresses this gap by systematically optimizing guardbands for metropolitan CV-QKD where FWM suppression is most impactful. We employ the coexistence model [7] to perform parameter sweeps of guardband size, classical power, and distance. We demonstrate that band-edge quantum channel placement with a guardband of 100–150 GHz maximizes SKR while minimizing classical capacity loss. This finding provides a critical design rule for practical deployment.

## 2. Analytical Model and Framework

In Gaussian-modulated CV-QKD under collective attacks with reverse reconciliation, the achievable SKR is

$$\text{SKR} = \beta I_{AB} - \chi_{BE}, \quad (1)$$

where  $\beta$  is the reconciliation efficiency,  $I_{AB}$  is the mutual information between Alice and Bob, and  $\chi_{BE}$  is the Holevo bound calculated from the symplectic eigenvalue of Eve's covariance matrices [9].

Excess noise quantifies all noise contributions beyond quantum shot noise that degrade the quantum signal, including transmitter imperfections, phase noise, and interference from external sources. In coexistence scenarios, nonlinear interference from co-propagating classical channels becomes the dominant contributor to excess noise. The excess noise parameter  $\xi_B$  (in shot-noise units) is calculated as [4]

$$\xi_B = P_{\text{int}} / (T \cdot h \cdot f \cdot B_s), \quad (2)$$

where  $P_{\text{int}}$  is the total interference power integrated over the quantum signal bandwidth  $B_s$ ,  $T = e^{-\alpha L}$  is the channel transmittance ( $\alpha$  is fiber attenuation,  $L$  is distance),  $h$  is Planck's constant and  $f$  is the optical frequency. In this work,  $\xi_B$  quantifies the excess noise contribution from co-propagating classical channels, where  $P_{\text{int}}$  includes nonlinear interference from FWM and SpRS, which generate noise within the quantum channel bandwidth and cannot be suppressed through optical filtering.

To assess the impact of distinctive nonlinear sources, we employ the comprehensive coexistence model from [7], which simultaneously evaluates FWM and SpRS interference through coupled power evolution equations along the fiber. The model accounts for the frequency-dependence of all relevant parameters, where the interference variance in single-mode fibers at the  $i^{\text{th}}$  frequency channel accumulates according to

$$\frac{dP_i^{\text{int}}(z)}{dz} = -\underbrace{\alpha_i P_i^{\text{int}}(z)}_{\text{Loss}} + \sum_{h \neq i} \eta_{ih} P_h(z) + \frac{16\gamma^2}{81} \left[ \sum_{\substack{f_h \neq f_i \\ f_k = 2f_h - f_i}} \underbrace{(\Phi_h + 2) P_h^2(z) P_k(z) \rho_{ihkh}(z)}_{\text{Degenerate FWM}} + 4 \sum_{\substack{f_h \neq f_i, f_h \neq f_i \\ f_k = f_h + f_i - f_i}} \underbrace{P_h(z) P_k(z) P_l(z) \rho_{ihkl}(z)}_{\text{Non-degenerate FWM}} \right] \quad (3)$$

where  $P_h(z)$  is the  $h^{\text{th}}$  classical-channel longitudinal power profile,  $\eta_{ih}$  is the SpRS efficiency,  $\gamma$  is the nonlinear coefficient,  $\Phi_h$  is the excess kurtosis, and  $\rho_{ihkl}(z)$  is the FWM efficiency. The interference terms in (3) reveal how distinct physical mechanisms directly impact achievable SKR through excess noise  $\xi$  (2). FWM scales with the cube of classical power ( $\sim \gamma^2 P^3 L_{\text{eff}}^2$ ), where  $\gamma$  is the nonlinear coefficient and  $L_{\text{eff}}^2$  is the effective length. FWM decays sharply with frequency separation, through the phase-matching term  $\rho_{ihkl} \propto 1/(1 + (\Delta\beta L_{\text{eff}})^2)$ , where  $\Delta\beta \propto \beta_2 \Delta f^2$  [10, Chap. 10]. Therefore, by widening the guardband around the quantum channel, FWM is suppressed through the elimination of strongly phase-matched products, directly lowering  $\xi$  and recovering SKR. SpRS behaves fundamentally differently; it scales linearly with power ( $g_R P_{\text{cl}} L_{\text{eff}}$ ) [10, Chap. 8] and spreads over a wide  $\sim 40$  THz bandwidth, making it insensitive to gigahertz-scale guardbands.

The different power scalings create a power-regime-dependent transition where FWM overtakes SpRS as the dominant noise source, occurring at per-channel powers between -5 and 0 dBm in metropolitan DWDM systems. This transition establishes a clear design rule. Below this power level, SpRS dominates, and guardbands provide negligible SKR improvement while reducing classical capacity. Above, FWM dominates, and the use of 2–3 channel guardbands (100–150 GHz) around the quantum channel is found to be highly effective at suppressing interference. This enables substantial SKR recovery with minimal capacity loss. This analytical framework directly connects the fiber parameters ( $\gamma, \beta_2, g_R$ ) to the security performance, enabling guardband deployment decisions without costly iterative simulations.

### 3. Numerical Analysis and Guardband Optimization

To validate these predictions, we systematically sweep guardband size (0–10 channels), classical power (-4.5 to 0.5 dBm/ch, corresponding to approximately 15–20 dBm total), and distance (0–30 km) across an 88-channel DWDM grid (50 GHz spacing, 1530–1565 nm). The system parameters include fiber ( $\alpha = 0.2$  dB/km,  $\beta_2 = -21.7$  ps<sup>2</sup>/km,  $\gamma = 1.3$  W<sup>-1</sup>km<sup>-1</sup>), CV-QKD (modulation variance  $V_A = 8$ , homodyne detection efficiency  $\eta_b = 0.6$ , reconciliation efficiency  $\beta = 0.95$ , electronic noise variance  $V_{el} = 0.01$ , as typical experimental parameters [11]), and quantum channel at Ch 44 (band-center) or Ch 88 (band-edge). Classical capacity loss depends on the placement of the quantum channel: the band-center requires symmetric guardbands ( $\Delta C = 2N_{\text{GB}}/88 \times 100\%$ ), while the edge of the band requires only a unilateral guardband ( $\Delta C = N_{\text{GB}}/88 \times 100\%$ ), where  $N_{\text{GB}}$  is the guardband size expressed in channels.

Figure 1(a) separates FWM and SpRS contributions at -4.5 dBm/ch as a function of classical channel position across the 88-channel DWDM grid to identify dominant effects. FWM-only shows 15% lower SKR at band-center

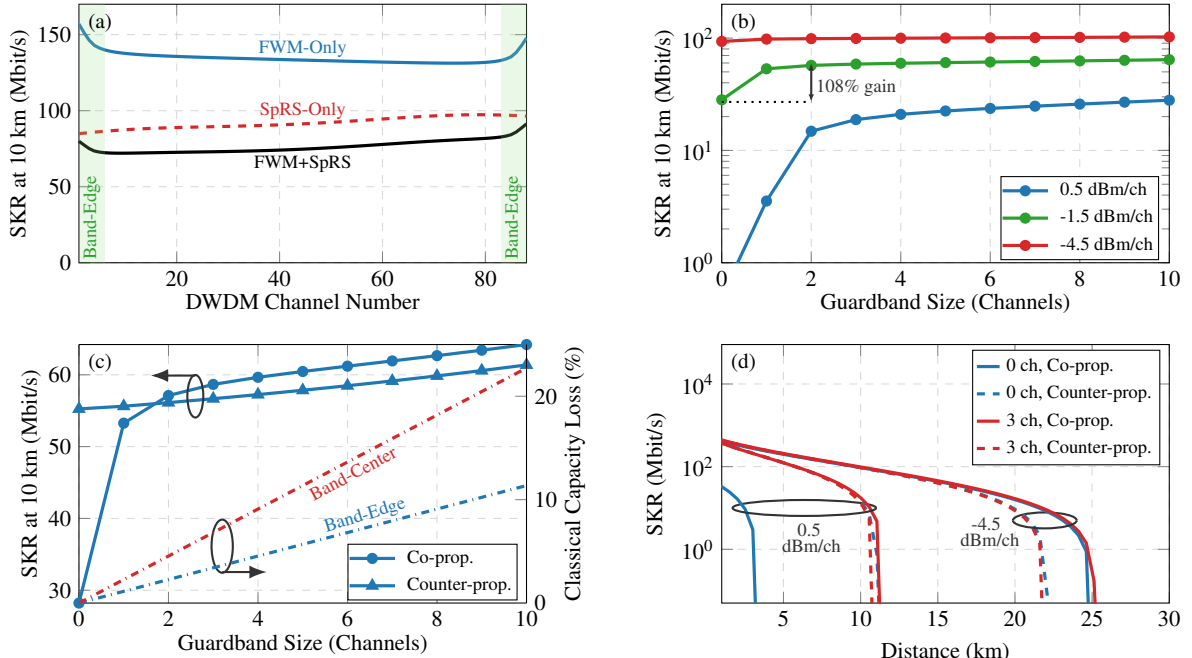


Fig. 1: (a) Spectral response at -4.5 dBm/ch showing FWM, SpRS, and combined effects. (b) Guardband effect across power regimes: 0.5 dBm/ch (blue), -1.5 dBm/ch (green), -4.5 dBm/ch (red). (c) SKR-capacity tradeoff at -1.5 dBm/ch for co-propagation (circles) and counter-propagation (squares). (d) Distance reach with/without 3-ch guardbands at high and low power.

versus band-edge due to reduced phase-matching. SpRS-only shows  $<10\%$  variation due to its broadband nature. The combined case follows the FWM profile offset by SpRS baseline. Based on this separation, the band-edge region (green, Ch 1–5 and Ch 83–88) is optimal for quantum channel deployment as it reduces FWM interference, even though the SpRS baseline remains. Within this region, we select Ch 88 as representative band-edge placement for subsequent guardband analysis. This insight supports the guardband optimization on power regimes as illustrated in Fig. 1(b).

Figure 1(b) reveals strong power-regime dependence. At high power (0.5 dBm/ch, 20 dBm total), FWM dominates: without guardbands, SKR drops to zero, but a 3-ch (150 GHz) guardband enables quantum communication with SKR of 38 Mbit/s. This reflects FWM’s cubic power dependence, which makes spectral separation crucial when launch powers are increased. In contrast, at low power ( $-4.5$  dBm/ch, 15 dBm total), SpRS dominates with SKR 195–205 Mbit/s regardless of guardband size. This shows that when broadband Raman scattering determines the noise floor, the advantage of spectral separation is minimal. In the intermediate regime ( $-1.5$  dBm/ch, 18 dBm total), a transitional behavior is observed. When the guardband widens from 0 to 3 ch, SKR increases by 108%. This transition confirms that the allocation of an optimal guardband must be adaptable: strict spacing is necessary for high-power links dominated by FWM to support quantum communication, while flexible spacing is needed for low-power links dominated by SpRS to preserve classical capacity.

Figure 1(c) quantifies the SKR-capacity tradeoff at  $-1.5$  dBm/ch. Consistent with Fig. 1(b), SKR curves (left axis) show co-propagation (co-prop.) gains 108% with 3-ch guardbands versus no-guardband baseline, while counter-propagation (counter-prop.) improves only 2.6% because opposite signal directions inherently suppress FWM phase-matching. Capacity loss (right axis) reveals band-edge advantage: unilateral protection (Ch 88: channels 85–87 removed) incurs 3.4% loss versus 6.8% for band-center symmetric protection (Ch 44: channels 41–43, 45–47 removed).

Fig. 1(d) demonstrates distance-power combinations. With 3-ch guardbands, both directions reach  $\sim 10$  km at 0.5 dBm/ch; without guardbands, co-propagation degrades to  $\sim 3$  km (70% decrease). At  $-4.5$  dBm/ch, all configurations achieve 20–23 km, confirming SpRS-limited operation where guardbands do not provide an advantage.

These results establish power-regime-dependent deployment strategies: band-edge placement with adaptive guardband allocation maximizes SKR while minimizing classical capacity loss. Unlike split-step Fourier simulations that require iterative wave propagation [8, 12], our approach enables rapid parameter sweeps across guardband configurations, classical powers, and distances, supporting network planning and SDN-controlled dynamic spectrum allocation in quantum-secure metropolitan DWDM networks.

#### 4. Conclusion

This work demonstrates that metropolitan-reach CV-QKD coexistence is practically achievable through analytical guardband optimization shaped by the FWM-SpRS power-regime transition. By exploiting the distinct frequency dependencies of these nonlinear effects, band-edge quantum channel placement with 150 GHz guardbands (Fig. 1(c)) enables 108% SKR improvement while incurring only 3.4% capacity loss, which is half the penalty of center-band symmetric protection. The analytical framework provides immediate deployment guidance for metropolitan DWDM networks: at high classical powers ( $> -1.5$  dBm/ch), 2–3 channel guardbands are essential for quantum operation; at low powers ( $< -4.5$  dBm/ch), guardbands sacrifice capacity without SKR benefit. This power-regime-dependent strategy eliminates costly iterative simulations, enabling network operators to optimize quantum-classical coexistence directly from fiber parameters ( $\gamma, \beta_2, g_R$ ) for practical deployment on existing metropolitan infrastructure.

#### Acknowledgement

This work was supported in part by the European Union’s Horizon Europe Research and Innovation Programme QuNEST Project under the Marie Skłodowska-Curie Grant Agreement No. 101120422

#### References

1. F. Bernd *et al.*, “A quantum access network,” *Nature* **501**, 69–72 (2013).
2. Y. Mao *et al.*, “Integrating quantum key distribution with classical communications in...” *Opt. Express* **26**, 6010 (2018).
3. A.A.E. Hajomer *et al.*, “Coexistence of continuous-variable quantum key...” arXiv preprint arXiv:2502.17388 (2025).
4. B. Qi *et al.*, “Feasibility of quantum key distribution through a dense wavelength...” *New J. Phys.* **12**, 103042 (2010).
5. R. Kumar *et al.*, “Coexistence of continuous variable QKD with intense DWDM...” *New J. Phys.* **17**, 043027 (2015).
6. S. Du *et al.*, “Impact of Four-Wave-Mixing Noise from Dense Wavelength...” *Phys. Rev. Appl.* **14**, 024013 (2020).
7. L. A. Zischler *et al.*, “Accurate and Effective Model for Coexistence...” arXiv preprint arXiv:2510.02807 (2025).
8. S. Moreolo *et al.*, “Continuous variable QKD in flexible optical...” *J. Opt. Commun. Netw.* **17**, B71–B82 (2025).
9. S. Pirandola and P. Papanastasiou, “Improved composable key rates for CV-QKD,” *Phys. Rev. Res.* **6**, 023321 (2024).
10. G. P. Agrawal, *Nonlinear Fiber Optics* (Academic Press, 2007), 5th ed.
11. J. dos Reis Frazão, “Co-propagation of Classical and Continuous-variable...” OFC pp. Th1C–5 (2024).
12. M. Iqbal *et al.*, “SDN-enabled CV-QKD and classical channels...” *J. Opt. Commun. Netw.* **17**, B28–B37 (2025).